Turkish Journal of Electrical Engineering & Computer Sciences

http://journals.tubitak.gov.tr/elektrik/

Research Article

Turk J Elec Eng & Comp Sci
(2017) 25: 735 – 751

doi:10.3906/elk-1506-64

Multitier decentralized control scheme using energy storage unit and load management in inverter-based AC microgrids

Sara NOUROLLAH*, Abolfazl PIRAYESH, Matthias FRIPP
Department of Electrical Engineering, Shahid Beheshti University, Tehran, Iran

Received: 07.06.2015 • **Accepted/Published Online:** 12.02.2016 • **Final Version:** 10.04.2017

Abstract: The use of renewable energies, such as wind and solar, is rising in microgrids. However, because of their intermittent nature, achieving a stable system in spite of the fluctuations of generation and demand is very difficult. Aiming to increase the stability margin of AC islanded microgrids comprising nondeterministic resources, properly share real power (P), and keep the network frequency (f) at nominal value, this study exploits the presence of energy storage units (ESUs) along with a load-shedding scheme. To this end, this study proposes a multitier decentralized control strategy that is based on frequency and includes three control schemes, distributed generation unit (DGU) control, ESU control, and local loads control (LLC). These controllers operate simultaneously. The DGU controller shares the loads among DGUs in accordance with the frequency droop method. On the other hand, the ESU controller controls the production of ESUs and also the LLCs manage the loads and dump-load of the microgrid. This method ensures the proper operation of AC microgrids that comprise intermittent resources under stand-alone conditions and despite numerous events. The time responses of P and f prove the high performance of the method. The simulations are performed and coded in m-file of MATLAB.

Key words: Energy storage unit, inverter-based microgrid, load management, multitier control scheme, nondeterministic resource

1. Introduction

A distributed power system in small scale that consists of loads, lines, and distributed generation units (DGUs) is called a microgrid [1,2]. A microgrid can be in two modes, stand-alone or grid-connected. The main components of an AC microgrid are as follows:

- Power suppliers with deterministic generation (e.g., battery, fuel cell, diesel generator, AC utility),
- Power suppliers with nondeterministic generation (e.g., wind turbine, photovoltaic),
- Variable and fixed loads,
- Energy storage unit (ESU) (e.g., supercapacitor, superconducting magnetic energy storage, compressed air energy storage).

The stability issue is vital for microgrids. A power system is considered stable if, after facing a physical disturbance, it can recover its equilibrium (i.e. a certain operation point) and most system variables are kept

*Correspondence: s_nourollah@sbu.ac.ir

within a permissible range [3]. The stability can be divided into three categories: small signal, transient, and voltage stability [3]. Several usual reasons for the instability of microgrids are as follows [4,5]:

- Energy limitation of DGUs,
- Failure of DGUs,
- Presence of intermittent resources (e.g., wind turbine, solar resource),
- Becoming islanded,
- Becoming grid-reconnected,
- Fluctuation of load (adding, shedding),
- Faults,
- Load dynamics (e.g., induction motors).

The stability of microgrids depends on important issues as follows:

- The operational mode of the microgrid (i.e. stand-alone and AC grid-connected) [6],
- The type of the used components in the network (i.e. power storage resources, unanticipated loads, intermittent resources) [1],
- The control structure of the energy generation.

Many studies concentrate on the problems of AC microgrids (e.g., detecting and processing of the islanded microgrid operation [7], power controlling and power-sharing in the inverter-based micro-grid [8]). In [9,10], different schemes were presented for improving the small signal stability and load-sharing. To do this, [10] proved the improvement of system operation using a compound scheme of conventional droop and average power equation. In contrast, [9] proposed a decentralized controller designed by resistive output impedance with no use of conventional droop for AC microgrids. For the inverter-based microgrids, many control structures have been presented (e.g., [4,11–13]). Majumder [4] presented instability types and their causes in AC microgrids. Furthermore, [11,13] explained a controller for improving two grid-connected and stand-alone operational modes by combining a droop controller with derivative and integral control blocks, respectively. In [12], two skilled plans, unit output power control and feeder flow control, for both operational modes of AC microgrids under different load conditions were described. In [7,14–17], the dynamic stability of the inverter-based microgrids was investigated. Pogaku et al. [7] improved the performance of autonomous AC microgrid operation using a droop control scheme in the state-space frame and Majumder et al. [15] used an auxiliary control loop.

When a fault occurs or a system becomes islanded, the system loads can play an important role to recover the system stability. Alaboudy et al. [14] dealt with this problem and studied the effects of RLC circuits and induction motors in inverter-based microgrids, while Magne et al. [18] focused on the stability and durability of MV multiload nonlinear microgrids (e.g., electric aircraft including several loads) and Weaver [19] assessed the effects of constant power loads on stability.

It is known that in wind and photovoltaic resources, the output power is not independent of the weather conditions. The fluctuations of these intermittent resources cause frequency and voltage deviations.

In order to share power and regulate voltage in an intermittent resource-based system, in [20], a control strategy without the use of a power storage system was implemented on a three-phase microgrid that comprised photovoltaic and diesel resources. However, in [21], the interaction of the use of energy storage elements and renewable energy resources in the stability of microgrids was analyzed and simulated. Datta et al. [22] studied this problem and presented a coordinated control scheme. For amending frequency fluctuations arising from renewable energy resources, Delille et al. [23] studied the presence of energy storages in wind and solar systems.

The presence of nondeterministic or intermittent resources in microgrids endangers the small signal stability, voltage and frequency regulation, and power-sharing and increases the vulnerability of the network [24]. Hence, the system will be forced to use ESUs [25] as a hydroelectricity-wind-pumped storage station [26] and fuel cells-hydrogen-pumped storage station [24] on the large scale and lead-acid battery on the small scale. However, in general, ESUs cannot be perfect elements because of having limitations (e.g., storage capacity, lifetime, environmental factors). References such as [16,23,25,26] focused on the presence of ESUs and also their problems (e.g., sizing, available capacity, how to charge and discharge). However, in AC distribution systems, the presence of an ESU is rarely seen to improve the stability margin.

For solving problems such as the energy shortage of deterministic generators, resources tripping, microgrid islanding, or load increasing, not only must ESUs interfere but also load-management (LM) must be added to the control structure [5,27]. Indeed, for preventing network collapse and ensuring competent performance of the microgrid, in particular during islanding mode, LM is necessary [5,16]. LM can be performed by a variety of methods [27,28]. Recently, extensive studies have been carried out on how to design and analyze the control structures in renewable-based smart-grids, such as in [29,30].

The objectives of this paper are the use of renewable energies and the compensation of their destructive effects on system stability. Hence, in order to maintain system stability, supply the network demands, and regulate parameters such as frequency, a multitier decentralized control (MTDC) scheme that includes three control subsections, DGU control, ESU control, and local load control, is proposed. In this strategy, the DGU-controller performs initial power-sharing based on the droop method among the DGUs and then other controllers, in order to maintain the system stability and decrease frequency fluctuations, make decisions about the status of the ESU and loads. This work proposes the use of the ESU without a communication link in distribution systems and a new nonlinear frequency droop characteristic for the ESU to tune the frequency response. The results prove that LM and the presence of ESUs lead to improve the microgrid operation against uncertainties and severe events.

The rest of this work is organized as follows: Section 2 describes the microgrid layout, which includes DGUs, loads, and ESU (with the proposed modes). In Section 3, the challenge of use of intermittent resources in microgrids and also the proposed control scheme with a mode diagram are developed. The case study with a scenario and the results of simulations are presented in section 4, followed by the conclusion in Section 5.

2. Microgrid layout

A microgrid consists of several important components such as intermittent and nonintermittent DGUs, ESUs, and loads. These components can have important effects on the operation of the distribution system and on the controller sections. Figure 1 demonstrates the schematic diagram of a microgrid.

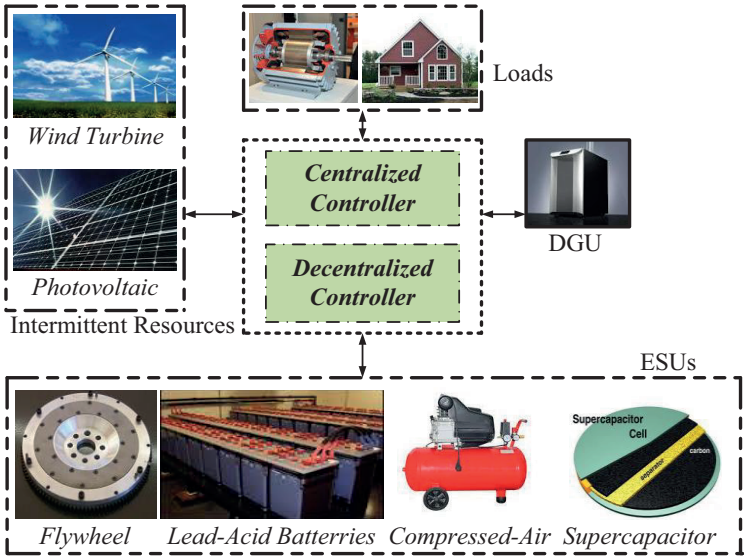

Figure 1. General schematic of a microgrid.

2.1. Deterministic and nondeterministic DGUs

In a distribution system, the initial energy resources exploited by DGUs can be available. A few examples of deterministic DGUs are diesel generators, fuel cells, and AC utilities. They generate the energy required by a network within a particular range (i.e. there are preset lower and upper limits). The amount of energy generated by a DGU is tunable. However, the energy of the renewable resources depends on the weather conditions and it is not always available or continuous in fixed amounts. Thus, if these energies are nonexistent or insufficient, the system operation would be disrupted.

2.2. Energy storage unit

In the power system, there are uncertainties such as faulty DGUs and lines, limited capacity of DGUs, and intermittent generation of renewable resources. The occurrence of these uncertainties would endanger the system stability and power-sharing. A solution is the use of ESUs.

2.3. Loads

A microgrid can have loads with different characteristics. An important point is to supply the power required by these loads. Indeed, since a network may not be able to supply all the demands, it is necessary to prioritize the loads for remaining in the network or being shed and this can be called LM. In this paper, for LM, first the loads will be prioritized, and then according to frequency deviations, the loads are shed or switched to the system in order of priority.

3. Proposed control scheme

The penetration of renewable energy resources is increasing. Because of their size limitation, they are used in microgrids.

In this study, the AC microgrid consists of some deterministic DGUs and also a nondeterministic DGU, which creates serious challenges for the system. Hence, in order to share loads and preserve parameters such

as voltage and frequency, a MTDC strategy is propounded for inverter-based microgrids, which consists of the following schemes:

- DGU control,
- ESU control,
- LM.

According to frequency and voltage droop characteristics proposed by previous studies [31,32], power changes cause voltage and frequency fluctuations. Hence, this study proposes the system frequency (f) as an input variable in the structure of controllers, which senses generation and demand variations in the network. In other words, the occurrence of events is identified using f.

In the first step of control, the DGU controller designed based on the droop method [16,31] shares power among the intermittent and nonintermittent DGUs for amending the stability margin of the system, regulating voltage, and maintaining f.

In the second step, dependent on f, the ESU controller switches the ESU to the system for compensating the lack of production. In the next step of stabilization, LM is done by the local load controllers (LLCs), which continuously receive f and use it to retain, shed, or return the network loads. In general, the dependence of MTDC on f is shown in Figure 2.

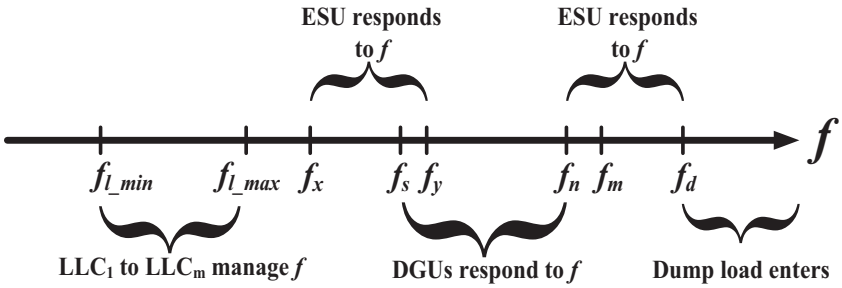

Figure 2. Dependence of proposed MTDC strategy on the system frequency.

3.1. DGU controller

In this study, the structure of the DGU controller is designed for inverter-based AC microgrids and is based on the droop method following [7]. The equations of inverter-based DGUs are given in the Appendix. In a normal situation (i.e. when the DGUs have the available generation capacity and operate properly, and the ESUs are on standby), the DGU controller continuously controls the system in order to supply all the network loads. Figure 3 shows the frequency droop characteristics of DGU-b$_i$ and DGU-b$_j$, where P_{max_DGUi} and P_{max_DGUj} are the maximum generation powers of DGUs.

3.2. ESU controller

If there are problems such as limited DGU capacity, DGU failure, or variable generation of renewable resources, then the ESU is needed.

In this work, three operational modes are defined for the ESU, which are as follows:

- **Standby mode (S-MODE):** In this mode, the ESU neither generates nor stores energy and waits for the ESU controller's commands.

- **Discharge mode (D-MODE):** If an uncertainty occurs, causing generation of insufficient energy in the system, the ESU enters D-MODE to generate power. In other words, power is shared among the DGUs and ESU according to the controller's command.

- **Charge mode (C-MODE):** If the energy stored in an ESU is not at maximum (e.g., because the ESU was previously in D-MODE), the unit starts to be charged as a load. Now the question is whether the ESU should take priority over the other loads in the network. A good approach would be for the ESU to enter C-MODE and be given top priority only if the energy stored in it (Q) reduces below 10% of the maximum capacity of the unit.

When the ESU operates, the amount of Q may vary and it affects the ESU controller decision. To this end, a control variable, C, is defined in accordance with Figure 4. This variable converts the integer value of Q to a numerical value. As can be seen in this figure, while decreasing Q, if it becomes less than 0.1 pu, then C will change from 1 to 0. However, for returning C to 1, Q should increase above 0.2 pu (a security hysteresis loop is formed). For $0.2 \leq Q \leq 0.9$, C equals 1 and $Q > 0.9$, where C is defined as 2.

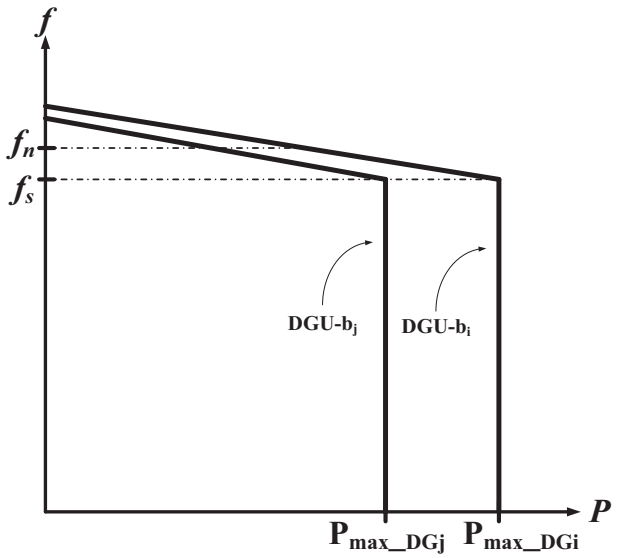

Figure 3. General frequency droop characteristics of DGUs.

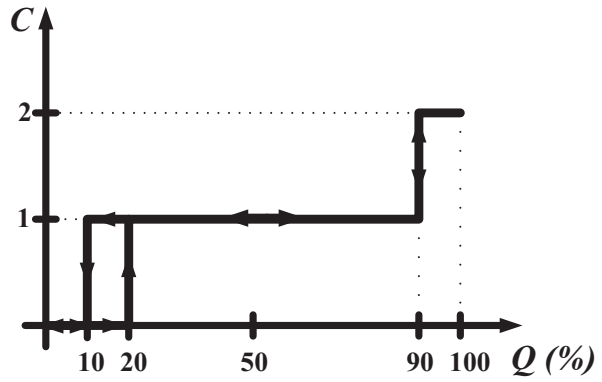

Figure 4. The value of C based on the energy stored in the ESU (Q).

In the ESU control scheme, whenever C equals 0, independent of f, the ESU should enter C-MODE (the ESU will operate as a load and, if needed, some loads should be shed).

In this controller, f is checked continuously. When f becomes less than f_y, the power generated by ESU (P_{ESU}) increases, and for $f < f_x$, the ESU generates its maximum energy (P_{max_ESU}), where f_x is defined as the upper limit frequency for $P_{ESU} = P_{max\_ESU}$. In D-MODE, for $f_x \leq f \leq f_y$, P_{ESU} increases and decreases in different curves. This discrepancy creates a safety margin during a change in the operational mode of the ESU and leads to the formation of a hysteresis loop. These curves are chosen based on an exponential

function in order to be able to adjust the decay rate using τ (e.g., if τ is selected near 0, these curves will be linear). The proposed nonlinear curve of P_{ESU} is obtained as in Eq. (1), where τ is a decay rate.

While increasing f from f_y to f_m, the ESU stays in S-MODE and does not produce energy. However, if an event occurs that causes the increasing of f more than f_m, then the ESU, dependent on C, stays in S-MODE (if C = 2) or switches to C-MODE (if C $\neq$ 2) and so the system should supply the needed energy of the ESU (P_{ch_ESU}). The ESU returns to S-MODE when the demand increases or the productions of DGUs decrease, which causes reduction of f below f_n. It is proposed that if Q $<$ 0.1 pu then the ESU takes priority over the other loads in the network. Indeed, the presence of the ESU makes a safety margin for the operation of the network in emergency status. If the remaining capacity of the ESU is near zero, then the lifetime of the ESU will be shortened. When Q $>$ 0.9 pu, it is proposed that the ESU leave C-MODE and the network is then ready for supplying highly prioritized loads. Inspired by previous work, usually because of the weather conditions and the existence of moisture in the air, a safety margin for the upper limit of ESU capacity is considered. Figure 5 shows the dependence of the ESU on two control signals, f and C. Generally, all DGUs and the ESU are droop-based. The frequency droop characteristics of DGUs are considered as conventional equations (linear functions). However, in order to operate the ESU in various modes, a new nonlinear frequency droop equation is proposed as in Figure 6.

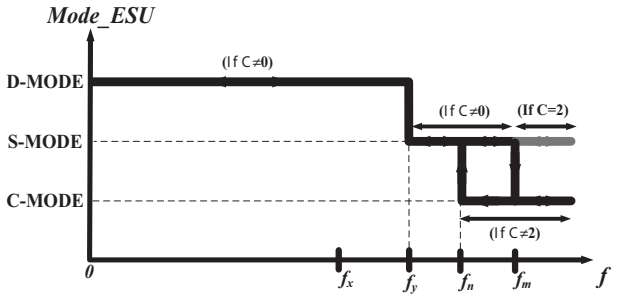

Figure 5. Dependence of ESU mode on f in ESU control scheme.

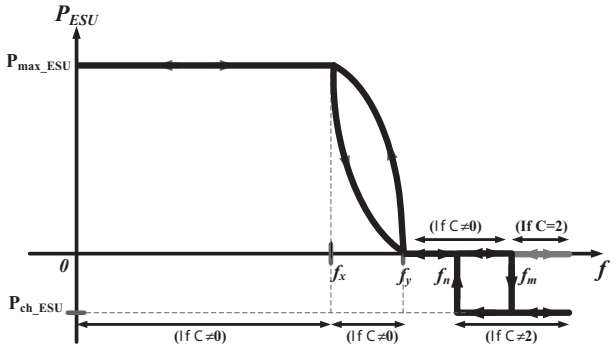

Figure 6. Proposed (P-f) droop characteristic of the ESU.

$$P_{ESU} = \begin{cases} P_{\max\_ESU} & f < fx \\ (P_{\max\_ESU}) \times (e^{\tau(f-fy)} - 1)/(e^{\tau(fx-fy)} - 1) & fx \leq f < fy \\ 0 & fy \leq f < fn \\ P_{ch\_ESU} \text{ or } 0 & fn \leq f \end{cases} \quad (1)$$

3.3. Local load controller

In order to enhance the network security margin, this paper suggests LLCs for the network loads and the dump-loads. Each load is equipped with a LLC and a relay to shed or return to the network; Figure 7 depicts the general schematic of a load with its controller. In this controller, f, as a control parameter, determines the load status in the network.

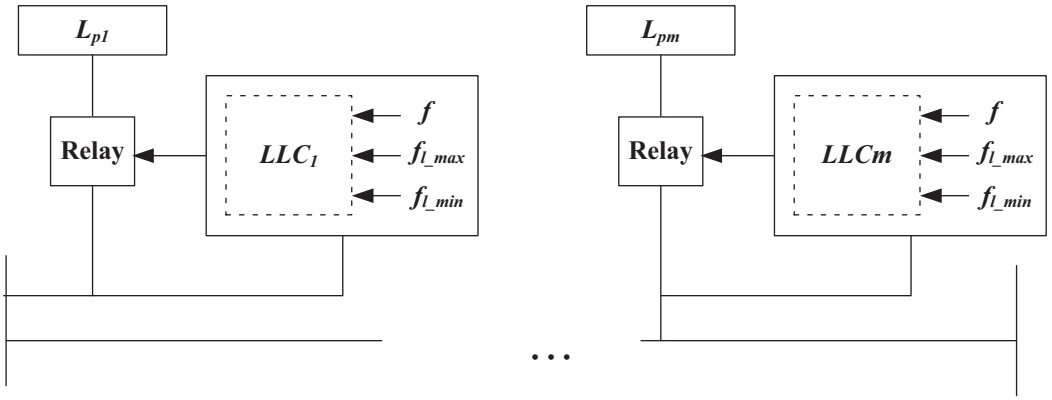

Figure 7. General schematic of load control scheme.

Whenever there are m prioritized loads ($L_{p1}, L_{p2}, \ldots, L_{pm}$) for shedding in the system, then m LLCs ($LLC_1, LLC_2, \ldots, LLC_m$) are contrived such that LLC_k sheds L_{pk} in $f = f_{l\_\max} - (k-1) \times df_l$ and returns it to the system in $f = f_{l\_\min} + (k \times df_r)$, where $k = 1, 2, \ldots, m$; $f_{l\_\min}$ and $f_{l\_\max}$ are the under and upper limit frequencies for LM; and df_l and df_r are obtained as in Eq. (2) and Eq. (3), respectively [1]. Figure 8 shows how to shed the loads.

$$dfl = \frac{fl_{\_\max} - fl_{\_\min}}{m-1} \tag{2}$$

$$dfr = 1.5dfl \tag{3}$$

3.4. Proposed mode diagram

Due to the LM and the presence of the ESU in the system, six operational statuses are defined as follows:

- S_a: ESU switches to S-MODE without load shedding (LSH).
- S_b: ESU switches to D-MODE without LSH.
- S_c: ESU switches to D-MODE with LSH.
- S_d: ESU switches to C-MODE with LSH.
- S_e: ESU switches to C-MODE without LSH.
- S_f: The system collapses.

In this study, probable events of a microgrid (ESU included) are classified as follows:

- E_0: without occurrence of a change.
- E_1: power shortage.
- E_2: additional power.
- E_3: Q reduced below 10%.

- E_4: Q increased above 20%.

- E_5: Q is more than 90%.

According to these defined statuses and events, a mode diagram is proposed and depicted in Figure 9.

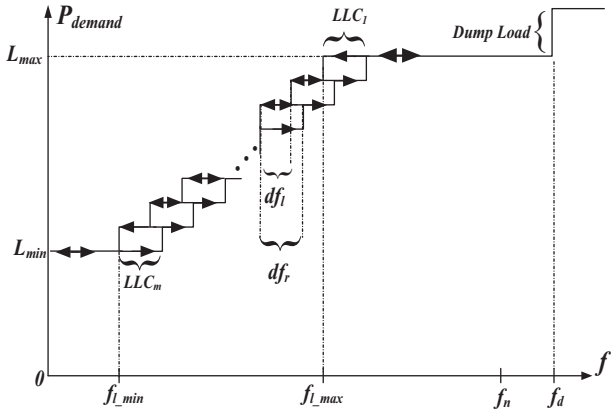

Figure 8. LM scheme done by LLCs.

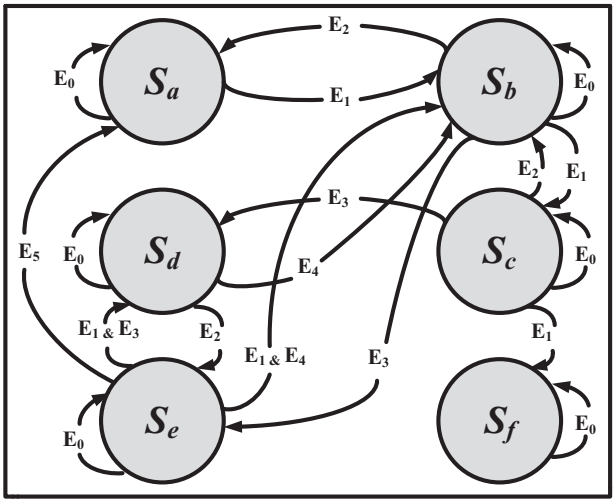

Figure 9. Proposed mode diagram of network.

It is assumed that the system is at first in S_a. If an event occurs (e.g., a DGU fails) and causes power shortage in the network (E_1), the system goes to S_b. If there is still shortage of power in the network, one or more of the LLCs commands LSH. In other words, the system switches to S_c.

If the Q gets below 0.1 pu (E_3), then the system enters either S_d (if there is at least a load to be shed) or S_e (when no load is shed).

Whenever the generation capacity of the network increases (E_2) (e.g., a faulty DGU is repaired and reenters the network, or there is a surge in the wind used by a turbine), then first the shed loads are returned to the system in order of priority, and then the ESU exits D-MODE.

If the system is in S_a and E_2 occurs, then, depending on C, the next status of the system is one of two statuses of S_a ($C = 2$) or S_e ($C \neq 2$).

It should be noted that when the ESU is charging (S_d or S_e), if a power shortage happens in the system (E_1), then the next status of the system depends on Q. If Q increases above 0.2 pu (E_4), then the ESU mode will be changed to D-MODE. Eventually, if the presence of the ESU and shedding of unnecessary loads cannot compensate the power shortage, the system will collapse (S_f).

4. Simulation and validation

In order to validate the proposed control system, a stand-alone AC microgrid is considered. This case, which is a five-bus system and consists of three deterministic inverter-based DGUs, a wind turbine, an ESU, and ten prioritized loads, is shown in Figure 10. Since the power generated by the wind turbine (P_{G-wind}) is unpredictable and uncontrollable, an energy generation curve is defined in Figure 11 like the one given in [28]. The details of the components are presented in Table 1.

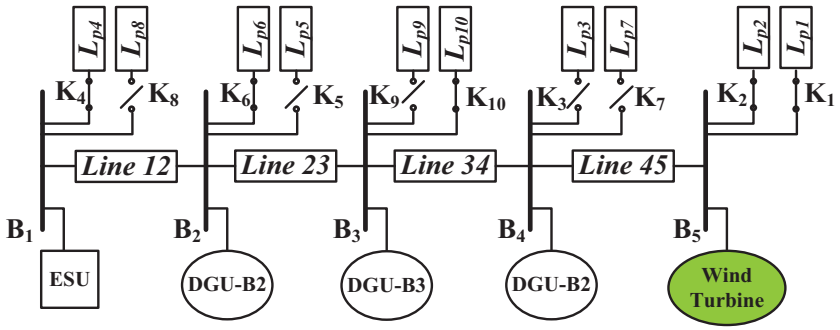

Figure 10. A schematic representation of the simulated microgrid.

Table 1. The system component details.

Producers	Maximum power (kW)
ESU	100
DGU-B2	350
DGU-B3	500
DGU-B4	160
Wind Turbine	Depends on wind intensity
Loads (in order of priority for shedding)	Consumption power (kW)
L_{p1}	50
L_{p2}	30
L_{p3}	40
L_{p4}	50
L_{p5}	90
L_{p6}	100
L_{p7}	160
L_{p8}	150
L_{p9}	175
L_{p10}	200
Lines	Impedance (Ω)
Line 12	0.3756 + j0.1936
Line 23	0.1878 + j0.0968
Line 34	0.1502 + j0.0774
Line 45	0.5634 + j0.2904

The system under consideration in this research is tested and simulated for a period of 50 s in duration. In this work, events happen such as load changes, generator failure, and variations in wind intensity. Three cases are defined in order to verify the performance of the proposed controller:

- Case A: a network that supplies all the loads without the use of the ESU and LM scheme.
- Case B: a network that supplies all the loads in the presence of the ESU but without the LM scheme.
- Case C: a network that is supported by the MTDC scheme.

In all three cases, at the initial time, switches K_1, K_2, K_4, K_6, and K_{10} are closed (Figure 10). Table 2 presents the events that will happen. The control parameters of the MTDC strategy are given in Table 3.

Table 2. Occurred events in the network.

t (s)	Event
3	L_{p4} exits
9	L_{p8} enters
13	DGU_b2 fails and then ESU starts
16	DGU-b4 starts and then ESU exits
18	L_{p7} enters and then ESU starts
22	L_{p5} enters and ESU arrives to P_{max_ESU} and then L_{p1} is shed
27	DGU-b2 starts and then ESU exits and shed L_{p1} returns
32	L_{p9} enters
35	L_{p3} enters and then ESU starts
38	ESU goes to C-MODE and then L_{p1} and L_{p2} are shed
40	L_{p9} exits and then shed L_{p1} and L_{p2} return
47	ESU is fully charged and goes to S-MODE

Table 3. The control parameters of the MTDC strategy.

f_n (HZ)	60
f_s (HZ)	59.95
f_x (HZ)	59.92
f_y (HZ)	59.95
$f_{l\_\max}$ (HZ)	59.91
$f_{l\_\min}$ (HZ)	59.82
df_l (HZ)	0.01
df_r (HZ)	0.015
P_{ch_ESU} (kW)	30
P_{max_ESU} (kW)	100
τ	± 20

4.1. Case A

In this case, the ESU and LM strategy are not used, so preservation of the network stability is very difficult.

According to Figure 11, because at the initial moment P_{G-wind} increases, all DGUs decrease their generation according to their droop coefficients and consequently f increases. In the period spanning 0 to 3 s, f changes from 59.962 Hz to 59.968 Hz and the total power generated by all generators ($P_{G-total}$) is equal to 455.2 kW.

As is seen in Table 2, L_{p4} exits at $t=$ 3 s, thereby causing the generation rate of the three DGUs to decrease and f to increase. At $t=$ 9s, L_{p8} enters the network, so f declines to 59.955 Hz and $P_{G-total}$ reaches 567.5 kW. The network is stable up to this point, as shown in Figure 12 and Figure 13. At $t=$ 13 s, DGU-b2 trips such that it forces the other DGUs to compensate the power deficiency. In consequence, f undergoes a sudden fall that leads to system tripping.

4.2. Case B

In this case, at necessary times, the ESU generates energy. Indeed, the presence of the ESU helps to stabilize the system. In $0 \leq t < 13$ (s), the results of Case B and Case A are similar. However, at $t=$ 13 s, unlike Case A, when DGU-b2 trips, the ESU goes to D-MODE immediately and begins to produce power ($P_{ESU} = 54$ kW). Hence, it prevents a drastic reduction of f ($f=$ 59.935 Hz). At t = 16 s, DGU-b4 starts to generate and

f increases, and so the ESU goes out. At this moment, the wind turbine produces 41.5 kW and therefore the DGU controller shares the rest of the load between DGU-b3 and DGU-b4. L_{p7} enters the network at t = 18 s and so f declines to 59.937 Hz and $P_{G-total}$ becomes 738.61 kW.

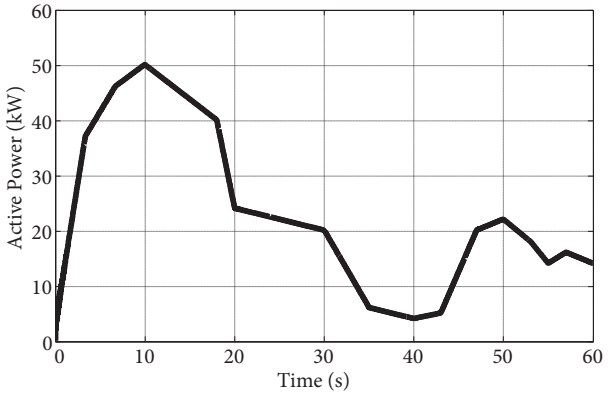

Figure 11. Proposed generation curve for wind turbine.

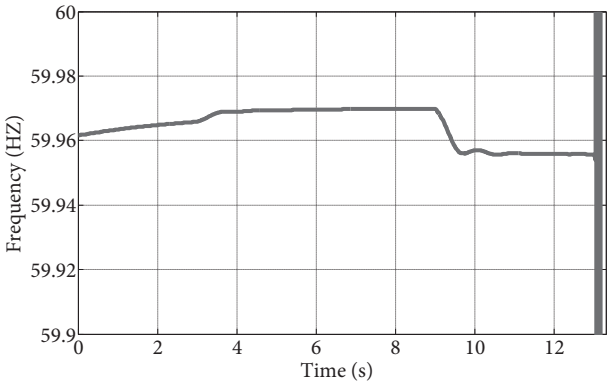

Figure 12. The microgrid frequency variation in Case A.

At t= 22 s, L_{p5} switches to the microgrid. At this time, the ESU has to produce $P_{D,\max}$, but it cannot prevent the f drop and therefore the system collapses, as shown in Figure 14. The power curves of the DGUs, wind turbine, and ESU are demonstrated in Figure 15.

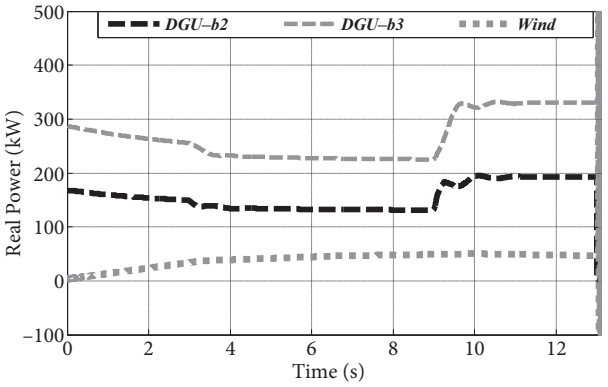

Figure 13. The generated real power by DGUs and wind turbine in Case A.

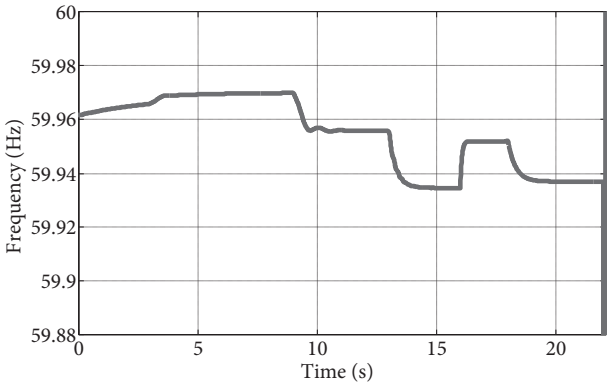

Figure 14. The microgrid frequency variation in Case B.

4.3. Case C

The ESU is exploited in this case and the loads are equipped with LLCs. In 0 $\leq t<$3 s, P_{G-wind} is increasing, as in Case A and Case B. Hence, the generation of DGU-b2 and DGU-b3 diminishes and thereby it causes the increase of f from 59.962 Hz to 59.964 Hz. Figure 16 depicts the frequency fluctuations in this case. It should be noted that in this period of time, the ESU is in S-MODE and the system status is S_a. At t= 3 s, L_{p4} is removed from the system, therefore leading $P_{G-total}$ to decrease to 406.05 kW and f to increase to 59.968 Hz; these values are cited in Table 4. At t= 9 s, L_{p8} switches to bus B_1 and then leads to $P_{G-total}$ = 567.5 kW and f = 59.955 Hz. At this moment, because of $f > 59.95Hz$, the ESU and the system status stay in S-MODE and S_a, respectively.

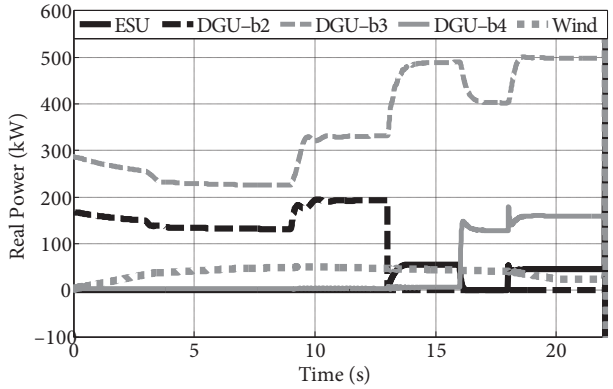

Figure 15. The generated real power by DGUs, wind turbine, and ESU in Case B.

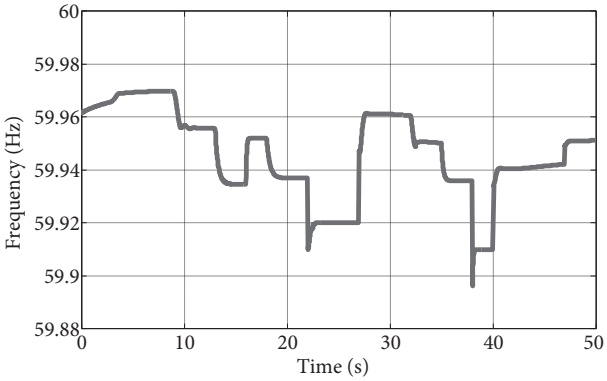

Figure 16. The microgrid frequency variation in Case C.

Table 4. The generation power of values of producers and the system frequency in Case C.

t (s)	f (Hz)	P_{DGU-b2} (kW)	P_{DGU-b3} (kW)	P_{DGU-b4} (kW)	P_{ESU} (kW)	P_{G-wind} (kW)	$P_{G-total}$ (kW)
0	59.962	167.7	287.5	0	0	0	455.2
3	59.968	137.87	233	0	0	35.18	406.05
9	59.955	195.4	322.1	0	0	50	567.5
13	59.935	0	487	0	54	46	587
16	59.952	0	400	127.37	0	41.5	568.87
18	59.937	0	497.5	159.37	44.74	37	738.61
22	59.91→59.92	0	497.5	159.37	98	23.6	778.47
27	59.961	281.92	402.76	131.16	0	20.7	836.54
32	59.952	347.07	497.1	157.83	0	13.56	1015.56
35	59.936	349	497	158	50.14	6	1060.14
38	59.898→59.91	345.1	496	156.8	–30	5	1002.9
40	59.941	310.81	444.2	141.3	–30	4.77	901.08
47	59.951	292.33	417.6	133	0	22.5	865.43

At t= 13 s, while P_{G-wind} goes down, DGU-b2 trips and then DGU-b3 increases its production, thus causing the frequency reduction to less than 59.95 Hz, and then the ESU will begin to produce power (54 kW), as in Case B. At this time, according to Figure 8, the system goes from S_a to S_b.

At t = 16 s, DGU-b4 switches to the microgrid. Thus, the DGU controller shares the demanded power between DGU-b3 and DGU-b4. At the same time, the ESU controller switches the ESU to S-MODE because of the increase in frequency.

At t= 18 s, L_{p7} enters and the ESU turns on again, and thus f varies to 59.937 Hz and $P_{G-total}$ is 738.61 kW. In this situation, the wind intensity reduction is the other reason for the frequency drop.

Similar to Case B, at t = 22 s, L_{p5} switches to the system, which leads to a sudden drop in f (from 59.937 Hz to 59.91 Hz). Therefore, LLC_1 sends a command signal to the corresponding relay for shedding L_{p1}. Hence, the system status changes to S_c. Accordingly, by shedding L_{p1}, f increases to 59.92 Hz.

At t= 27 s, the repaired DGU-b2 returns to the system and so the power generations of other DGUs decrease. Because f becomes more than 59.925 Hz (59.91 + 0.015), hence the shed L_{p1} returns to the system by the command of LLC_1.

At t = 32 s, switching L_{p9} to the system causes a frequency drop from 59.961 Hz to 59.952 Hz. Figures 16 and 17 demonstrate f and the generated power of the resources, respectively.

Due to adding L_{p3} to the system and hence the frequency reduction at t = 35 s, the ESU injects power into the system (P_{ESU} = 50.14 kW). However, at t = 38 s, Q falls below 20% (e_3) and therefore the ESU mode changes from D-MODE to C-MODE regardless of the power shortage in the system. Note that when the ESU is in C-MODE, it treats it like a load. Hence, at t= 38 s, the DGUs raise their generation and f decreases to 59.898 Hz. At this moment, L_{p1} and L_{p2} are shed and f goes to 59.91 Hz. As mentioned in Table 2, at t= 40 s L_{p9} exits and so f becomes more than 59.925 Hz. Therefore, at t= 40 s, L_{p1} and L_{p2} return to the network.

As can be seen in Figure 17, the wind intensity does not vary in $38 \leq t < 43\,s$, but at t= 43 s it begins to increase such that it improves f.

At t= 47 s, the ESU is fully charged and the ESU mode varies from C-MODE to S-MODE, and hence the total load of the system decreases and subsequently f and $P_{G-total}$ will be equal to 59.951 Hz and 865.43 kW, respectively. The system status is illustrated in Figure 18.

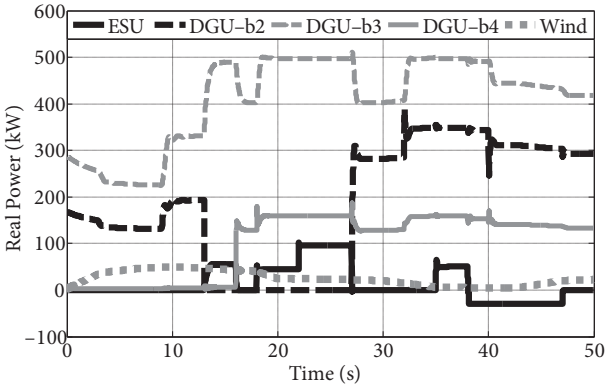

Figure 17. The generated real power by DGUs, wind turbine, and ESU in Case C.

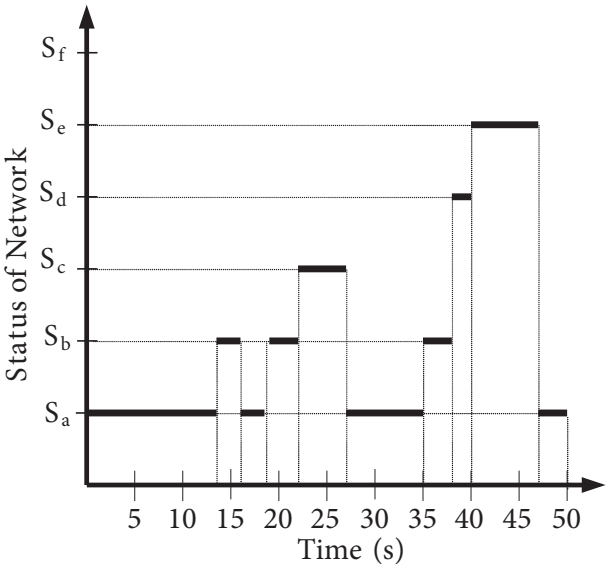

Figure 18. The system status in Case C.

As can be concluded from the results, the proposed controller can stabilize AC microgrids using the ESU and managing the loads for power-sharing and f regulation against destructive and numerous events and uncertainties.

5. Conclusion

In this study, a MTDC scheme is proposed for an AC stand-alone inverter-based microgrid that consists of a nondeterministic energy resource, an ESU, and three VSI-based DGUs with variable demands. This strategy comprises three controllers, a DGU controller, an ESU controller, and LLCs. These control sections operate simultaneously. For assessing the performance of the proposed method, three cases are considered that share the power among generation units and endeavor to maintain f at nominal frequency. These cases are as follows:

- Stability preservation and power management using just VSI-based DGUs,

- Stability preservation and power management using VSI-based DGUs in the presence of the ESU,

- Stability preservation and power management using the LSH strategy for better use of the ESU and VSI-based DGUs.

In this controller, f is used as an input parameter. Indeed, the controllers trace the frequency deviations and then immediately decide the next status of the system. The simulations coded and obtained in the MATLAB environment prove the improved operation of the AC microgrid against uncertainties and various events.

Nomenclature

Abbreviations

ESU	Energy storage unit
LSH	Load shedding
MTDC	Multitier decentralized control
DGU	Distributed generation units
LLC	Local loads control
P	Real power
LM	Load management
S-MODE	Standby mode
D-MODE	Discharge mode
C-MODE	Charge mode
E	Event
S	Status

Parameters and variables

t	Time
P_{max_DGUj}	The maximum generation power of the ith DGU
P_{ESU}	The power generated by the ESU
P_{max_ESU}	The maximum power generated by the ESU
P_{ch_ESU}	The power absorbed by the ESU in C-MODE
f_n	The nominal frequency
f_x, f_y	The lower and upper limit frequencies for the ESU in D-MODE
f_m	The lower limit frequency for switching the ESU to C-MODE
$\tau\tau$	Decay rate
L_{pi}	The ith prioritized load
$f_{l\_\min}$ and $f_{l\_\max}$	The lower and upper limit frequencies for load shedding
P_{G-wind}	The power generated by the wind turbine

References

[1] Xu L, Chen D. Control and operation of a DC microgrid with variable generation and energy storage. IEEE T Power Deliver 2011; 26: 2513-2522.

[2] Hatziargyriou N, Asano H, Iravani R, Marnay C. Microgrids. IEEE Power Energy M 2007; 5: 78-94.

[3] IEEE/CIGRE Joint Task Force on Stability Terms and Definitions. Definition and classification of power system stability. IEEE T Power Syst 2004;19: 1387-1401.

[4] Majumder R. Some aspects of stability in microgrids. IEEE T Power Syst 2013; 28: 3243-3252.

[5] Chen D, Xu L, Yao L. DC Voltage variation based autonomous control of DC microgrids. IEEE T Power Deliver 2013; 28: 637-648.

[6] Mehrizi-Sani A, Iravani R. Potential-function based control of a microgrid in islanded and grid-connected modes. IEEE T Power Syst 2010; 25: 1883-1891.

[7] Pogaku N, Prodanovic M, Green TC. Modeling, analysis and testing of autonomous operation of an inverter-based microgrid. IEEE T Power Electr 2007; 22: 613-625.

[8] Chung IY, Liu W, Cartes DA, Collins EG, Moon SI. Control methods of inverter-interfaced distributed generators in a microgrid system. IEEE T Ind Appl 2010; 46:1078-1088.

[9] Guerrero JM, Matas J, Garciade VL, Castilla M, Miret J. Decentralized control for parallel operation of distributed generation inverters using resistive output impedance. IEEE T Ind Electron 2007; 54: 994-1004.

[10] Marwali MN, Dai M, Keyhani A. Stability analysis of load sharing control for distributed generation systems. IEEE T Energy Convers 2007; 22: 737-745.

[11] Kim J, Guerrero JM, Rodriguez P, Teodorescu R, Nam K. Mode adaptive droop control with virtual output impedances for an inverter-based flexible AC microgrid. IEEE T Power Electr 2011; 26: 689-701.

[12] Ahn S, Park J, Chung I, Moon S, Kang S, Nam S. Power sharing method of multiple distributed generators considering control modes and configurations of a microgrid. IEEE T Power Deliver 2010; 25: 2007-2016.

[13] Salamah AM, Finney SJ, Williams BW. Autonomous controller for improved dynamic performance of AC grid, parallel-connected, single-phase inverters. IET Gener Transm Dis 2008; 2: 209-218.

[14] Alaboudy AHK, Zeineldin HH, Kirtley JL. Microgrid stability characterization subsequent to fault-triggered islanding incidents. IEEE T Power Deliver 2012; 27: 658-669.

[15] Majumder R, Chaudhuri B, Ghosh A, Majumder R, Ledwich G, Zare F. Improvement of stability and load sharing in an autonomous microgrid using supplementary droop control loop. IEEE T Power Syst 2010; 25: 796-808.

[16] Divshali PH, Alimardani A, Hosseinian SH, Abedi M. Decentralized cooperative control strategy of microsources for stabilizing autonomous VSC-based microgrids. IEEE T Power Deliver 2012; 27: 1949-1959.

[17] Radwan AAA, Mohamed YARI. Linear active stabilization of converter-dominated DC microgrids. IEEE T Smart Grid 2012; 3: 203-216.

[18] Magne P, Nahid-Mobarakeh B, Pierfederci S. General active global stabilization of multi-loads DC-power networks. IEEE T Power Electr 2012; 27: 1788-1798.

[19] Weaver WW. Dynamic energy resource control of power electronics in local area power networks. IEEE T Power Electr 2011; 26: 852-859.

[20] Elmitwally A, Rashed M. Flexible operation strategy for an isolated PV-diesel microgrid without energy storage. IEEE T Energy Conver 2011; 26: 235-244.

[21] Zhixin M, Domijan A, Lingling F. Investigation of microgrids with both inverter interfaced and direct AC-connected distributed energy resources. IEEE T Power Deliver 2011; 26: 1634-1642.

[22] Datta M, Senjyu T, Yona A, Funabashi T, Chul-Hwan K. A coordinated control method for leveling PV output power fluctuations of PV-diesel hybrid systems connected to isolated power utility. IEEE T Energy Convers 2009; 24: 153-162.

[23] Delille G, François B, Malarange G. Dynamic frequency control support by energy storage to reduce the impact of wind and solar generation on isolated power system's inertia. IEEE T Sustainable Energy 2012; 3: 931-939.

[24] Zhou T, Francois B. Energy management and power control of a hybrid active wind generator for distributed power generation and grid integration. IEEE T Ind Electron 2011; 58: 95-104.

[25] Mitra J, Vallem M R. Determination of storage required to meet reliability guarantees on island-capable microgrids with intermittent sources. IEEE T Power Syst 2012; 27: 2360-2367.

[26] Papaefthymiou SV, Karamanou E, Papathanasiou S, Papadopoulos M. A wind-hydro-pumped storage station leading to high RES penetration in the autonomous island system of Ikaria. IEEE T Sustainable Energy 2010; 1: 163-172.

[27] Wang B, Sechilariu M, Locment F. Intelligent DC microgrid with smart grid communications: control strategy consideration and design. IEEE T Smart Grid 2012; 3: 2148-2156.

[28] Wu T, Yang Q, Bao Zh, Yan W. Coordinated energy dispatching in microgrid with wind power generation and plug-in electric vehicles. IEEE T Smart Grid 2013; 4: 1453-1463.

[29] Lu D, Kanchev H, Colas F, Lazarov V, François B. Energy management and operational planning of a microgrid with a PV-based active generator for smart grid applications. IEEE T Ind Electron 2011; 58: 4583-4592.

[30] Locment F, Sechilariu M, Houssamo I. DC load and batteries control limitations for photovoltaic systems; experimental validation. IEEE T Power Electr 2012; 27: 4030-4038.

[31] Rokrok E, Golshan MEH. Adaptive voltage droop scheme for voltage source converters in an islanded multibus microgrid. IET Gener Transm Dis 2010; 4: 562-578.

[32] Majumder R, Ghosh A, Ledwich G, Zare F. Load sharing and power quality enhanced operation of a distributed microgrid. IET Renew Power Gen 2009; 3: 109-119.

Appendix.

Equations of inverter-based DG unit controller.

Voltage controller:

$$\begin{cases} i_{ld}^{*} &= Fi_{od} - \omega_n C_f v_{oq} + k_{pv}\left(v_{od}^{*} - v_{od}\right) \\ & \quad + k_{iv}\int\left(v_{od}^{*} - v_{od}\right)dt \\ i_{lq}^{*} &= Fi_{oq} + \omega_n C_f v_{od} + k_{pv}\left(v_{oq}^{*} - v_{oq}\right) \\ & \quad + k_{iv}\int\left(v_{oq}^{*} - v_{oq}\right)dt \end{cases} \tag{A-1}$$

Current controller:

$$\begin{cases} v_{id}^{*} &= -\omega_n L_f i_{lq} + k_{pc}\left(i_{ld}^{*} - i_{ld}\right) \\ & \quad + k_{ic}\int\left(i_{ld}^{*} - i_{ld}\right)dt \\ v_{iq}^{*} &= +\omega_n L_f i_{ld} + k_{pc}\left(i_{lq}^{*} - i_{lq}\right) \\ & \quad + k_{ic}\int\left(i_{lq}^{*} - i_{lq}\right)dt \end{cases} \tag{A-2}$$

Power controller:

$$\begin{cases} p = v_{od}i_{od} + v_{oq}i_{oq} \\ q = v_{od}i_{oq} - v_{oq}i_{od} \end{cases} \tag{A-3}$$

$$\begin{cases} P = \frac{\omega_c}{S+\omega_c}p \\ Q = \frac{\omega_c}{S+\omega_c}q \end{cases} \tag{A-4}$$

$$\begin{cases} \omega_{com} = \omega_n - m.P \\ v_{od}^{*} = v_n - n.Q \\ v_{oq}^{*} = 0 \end{cases} \tag{A-5}$$

Filtering system:

$$\begin{cases} i_{ld}^{\bullet} = -\frac{r_f}{L_f}i_{ld} + \omega_{com}.i_{lq} + \frac{1}{L_f}(v_{id}^{*} - v_{od}) \\ i_{lq}^{\bullet} = -\frac{r_f}{L_f}i_{lq} - \omega_{com}.i_{ld} + \frac{1}{L_f}(v_{iq}^{*} - v_{oq}) \end{cases} \tag{A-6}$$

$$\begin{cases} v_{od}^{\bullet} = \omega_{com}.v_{oq} + \frac{1}{C_f}\left(i_{ld} - i_{od}\right) \\ v_{oq}^{\bullet} = -\omega_{com}.v_{od} + \frac{1}{C_f}\left(i_{lq} - i_{oq}\right) \end{cases} \tag{A-7}$$

$$\begin{cases} i_{od}^{\bullet} = -\frac{r_c}{L_c}i_{od} + \omega_{com}.i_{oq} + \frac{1}{L_c}\left(v_{od} - v_{bd}\right) \\ i_{oq}^{\bullet} = -\frac{r_c}{L_c}i_{oq} - \omega_{com}.i_{od} + \frac{1}{L_c}\left(v_{oq} - v_{bq}\right) \end{cases} \tag{A-8}$$

Where:

$r_{f,}L_{f,}C_f$	the per-phase resistance, inductance, and capacitance of the LC filter of the filtering system
$r_{c,}\, L_c$	the per-phase resistance and inductance of the coupling inductor of the filtering system
p, q	the injected instantaneous real and reactive powers
v_o, i_o	the output voltage and current of the inverter-based DG unit
P, Q	the real and reactive powers of the fundamental component
ω_c	the filter cutoff frequency
ω_{com}	the fundamental voltage frequency
ω_n, v_n	the nominal frequency and voltage
v_o^*	the output voltage reference
m, n	the droop coefficients
i_l^*	the reference current in the current controller
F	the feed forward gain in the voltage controller
k_{pv}, k_{iv}	the proportional and integral gains in the voltage controller
v_i^*	the reference voltage of the filtering system
i_l	the current of $L_f L_f L_f$
k_{pc}, k_{ic}	the proportional and integral gains in the current controller